LHCb–2003–126
Physics
3^{rd} November 2003

Exclusive Selection of $B_d^0 \to D^{*-}\pi^+$

L.R. Allebone and U. Egede
Imperial College London
The Blackett Laboratory, London SW7 2BZ

Abstract

The decay $B_d^0 \to D^{*-}\pi^+$ provides a theoretically clean system to access the CKM angle γ. The mode suffers no penguin or loop contributions and is therefore expected to be robust against New Physics beyond the Standard Model. Consequently the measurement of γ determined from this decay mechanism offers a benchmark for other γ yielding channels that are sensitive to non–Standard Model processes.

A Monte Carlo simulation of the reconstruction of the exclusive $B_d^0 \to D^{*-}\pi^+$ decay using the LHCb physics analysis software, DaVinci, is described. Physics performance studies show that an annual untagged and triggered signal yield of (206$\pm$9) k exclusive $B_d^0 \to D^{*-}\pi^+$ events and a combinatorial $b\overline{b}$ background–to–signal ratio of less than 0.3 is forecast for LHCb.

1 Introduction

The Standard Model (SM) with three quark generations allows the manifestation of CP violation in both the weak and the strong interactions. CP asymmetry in the weak sector arises from the complex phases of the three–by–three unitary CKM matrix. Physics beyond the Standard Model may also prove responsible for the phenomenon. Understanding the non–invariance of the CP symmetry could lead to an insight into the underlying processes of fermion mass generation and flavour mixing.

The Standard Model predicts large complex phases in the b–quark system. The LHCb experiment will exploit the copious number of $b\overline{b}$ pairs produced at the LHC in order to perform precision measurements of CP asymmetries and rare decays with the large number of B–meson decay modes available[1] [1].

The $B_d^0 \to D^{*-}\pi^+$ decay is one such accessible channel of the LHCb experiment that will be used to determine the CKM angle γ [2]. This mode, being robust against penguin contributions, provides a theoretically pure manner to extract the angle [3]. Therefore the γ measurement established with this system can be used as a Standard Model reference to compare the results of other decays that are more susceptible to New Physics; an example being γ extracted from a time dependent analysis of $B_d^0 \to \pi^+\pi^-$ and $B_s^0 \to K^+K^-$ [4].

2 The LHCb Physics Analysis Framework

The LHCb physics analysis software application, DaVinci, is an object orientated environment based on the Gaudi framework. DaVinci is a high level physics analysis package that provides the tools for the processing of both real and Monte Carlo LHCb data. The application allows the performance of the reconstruction, the trigger decisions and the offline selections of various decay channels to be assessed.

To determine the reconstruction potential of the decay mode $B_d^0 \to D^{*-}\pi^+$ at LHCb, the following samples of Monte Carlo events were generated and analysed [5]:

- A $B_d^0 \to D^{*-}\pi^+$ exclusive signal sample of 49.5k events generated inside an opening angle of 400mrad. The events correspond to a phase space acceptance of $\varepsilon_b = 0.3471 \pm 0.0003$.

[1] The LHC will be an abundant source of b–hadrons owing to the high luminosity and the large $b\overline{b}$ cross section for 14 TeV proton–proton collisions of ~ 500 μbarn.

- A sample of approximately 10^7 inclusive $b\overline{b}$ events were generated inside an opening angle of 400mrad and correspond to a phase space acceptance of $\varepsilon_{bb} = 0.4321 \pm 0.0004$. The events were used in the estimation of the combinatorial background for this decay channel.

- A sample of approximately 3x10^7 minimum bias events that were used for trigger studies.

3 Exclusive Reconstruction of $B_d^0 \to D^{*-}\pi^+$ at LHCb

Using the DaVinci framework, three algorithms were written to evaluate the performance of the reconstruction of the exclusive $B_d^0 \to D^{*-}\pi^+$, $D^{*-} \to \overline{D^0}\pi^-$, $\overline{D^0} \to K^+\pi^-$ decay chain[2]. A series of selection cuts were applied to the particle candidate formed by the decay product combination in order to determine the true particle aggregations. The reconstruction algorithms were optimised to maximise $S/\sqrt{S+B}$ where S is the number of signal events selected per year before trigger and B is the number of combinatorial $b\overline{b}$ background events selected per year before the trigger is applied[3].

In order to reduce the amount of data analysed, a set of loose preselection cuts were applied to both the signal and background samples. This reduced the $b\overline{b}$ background sample to below 1% of its original size[4].

The ntuple outputs of the preselection trials were used as input to a stand–alone algorithm designed to determine the optimal $S/\sqrt{S+B}$ for this decay mode[5]. The optimised selection cuts are documented below.

In both the preselection and the optimised analyses the pions and Kaons were selected using the 'CombinedParticleMaker'. This DaVinci tool combines the information from the various subdetectors that provide the particle identification[6] to give a hypothesis on the identity of a particle. The tool was used in a non-exclusive selection mode resulting in some tracks being marked

[2]The pion from the $B_d^0 \to D^{*-}\pi^+$ decay is known as the 'fast' pion and the pion from the $D^{*-} \to \overline{D^0}\pi^-$ decay is known as the 'slow' pion.

[3]It was decided to optimise the reconstruction algorithms before application of the LHCb trigger criterion so not to reduce the data sample size. It is assumed that the trigger efficiency for the signal and selected background after all selection criteria are applied are the same.

[4]Half of the inclusive $b\overline{b}$ background data sample was reserved in order to have an unbiased data sample on which to test the 'optimised' selection criteria.

[5]Each selection criteria was defined within a range and a number of iterations set; the optimising algorithm then determined the collection of cuts with an optimal $S/\sqrt{S+B}$.

[6]i.e the RICH, calorimeter and muon systems

as both pion and Kaon. Every particle was identified as a pion and particles with a $\Delta lnL_{K\pi} > -5.0$, based on the RICH information, were also marked as Kaon. No other selection cut was made on the pion or Kaon tracks before the Kaon PID selection criteria in the offline analysis. The track quality was defined by the standard track definitions at the Brunel[7] reconstruction stage [6].

3.1 Upstream Tracks

The main LHCb tracking system consists of four tracking stations; the most upstream station is known as the Trigger-Tracker (TT) station and is located between RICH1 and the dipole magnet. There are a further three tracking stations, T1–T3, located between the dipole magnet and RICH2. The Vertex Detector (VELO) is also used for tracking. The track categories after reconstruction are:

- VELO tracks
- Upstream tracks, which are formed from hits in the VELO and the TT station
- Long tracks, which use hits from the VELO and all tracking stations
- Downstream tracks, which use hits from TT and T1–T3.

The most important track categories for the reconstruction of $B_d^0 \to D^{*-}\pi^+$ events are long and upstream tracks. The upstream tracks are particularly important in the reconstruction of slow pions. This is because the slow pion from the D^* decay is essentially at rest with respect to the D^* centre–of–mass frame as explained in section 3.3.1. Therefore the pion typically has a low momentum and will hence have a high curvature in the dipole magnet region. In some cases the curvature of the slow pion is such that the particle is lost outside of the LHCb detector acceptance and will not be recorded at the later tracking stations, T1–T3.

3.2 Optimised Selection Cuts

3.2.1 $\overline{D^0} \to K^+\pi^-$ Optimised Selection Cuts

- (Reconstructed D^0 mass - 1864) $< \pm$ 11 MeV/c^2

[7]Brunel is the LHCb software reconstruction package based on the Gaudi framework [7].

- Pion transverse momentum > 150 MeV/c
- Kaon transverse momentum > 200 MeV/c
- χ^2 of unconstrained K/π mass vertex fit < 40
- 0 mm $< D^0$ z–vertex position - 1^0 z–vertex position < 200 mm
- D^0 z–vertex position < 150 mm

3.2.2 $D^{*-} \rightarrow \overline{D^0}\pi^-$ Optimised Selection Cuts

- Slow pion impact parameter < 9 mm
- D^0 impact parameter < 8 mm
- D^0 transverse momentum > 50 MeV/c
- χ^2 of unconstrained D^0/π mass vertex fit < 15
- 143.75 MeV/c^2 $<$ (D^* - D^0) mass difference $<$ 147.25 MeV/c^2
- -40 mm $< D^*$ z–vertex position - 1^0 z–vertex position < 100 mm
- D^* z–vertex position < 150 mm

3.2.3 $B_d^0 \rightarrow D^{*-}\pi^+$ Optimised Selection Cuts

- (Reconstructed B_d^0 mass - 5728) $< \pm$ 200 MeV/c^2 [8]
- Fast pion impact parameter > 0.05 mm
- B_d^0 impact parameter < 0.05 mm
- Fast pion transverse momentum > 1300 MeV/c
- D^* transverse momentum > 1400 MeV/c
- χ^2 of unconstrained D^*/π mass vertex fit < 12
- 1 mm $< B_d^0$ z–vertex position - 1^0 z–vertex position < 50 mm
- (D^0 z–vertex position - B_d^0 z–vertex position) > 0 mm

[8] This selection cut is known as the 'loose' mass window. In addition a 'tight' B_d^0 mass window of (B_d^0 mass - 5728) $< \pm$ 50 MeV/c^2 was used.

3.3 Selection Cut Synopsis

The effect of the optimised D^* - D^0 mass difference, the B_d^0 z–vertex - primary z–vertex and the D^* transverse momentum selection criteria on the signal and background levels are demonstrated below.

3.3.1 D^* - D^0 Mass Difference Selection Cut

The pion from the $D^* \rightarrow D^0\pi$ decay is known as the 'slow' pion. The mass difference between the D^* and the D^0 is 145.4 MeV/c^2, which leaves only 5 MeV/c^2 after subtraction of the pion rest mass. Therefore the pion is essentially at rest in the D^* centre–of–mass frame of reference.

The mass difference between the D^* and the D^0 candidates provides a powerful cut for the rejection of the combinatorial $b\overline{b}$ background in the D^* reconstruction algorithm.

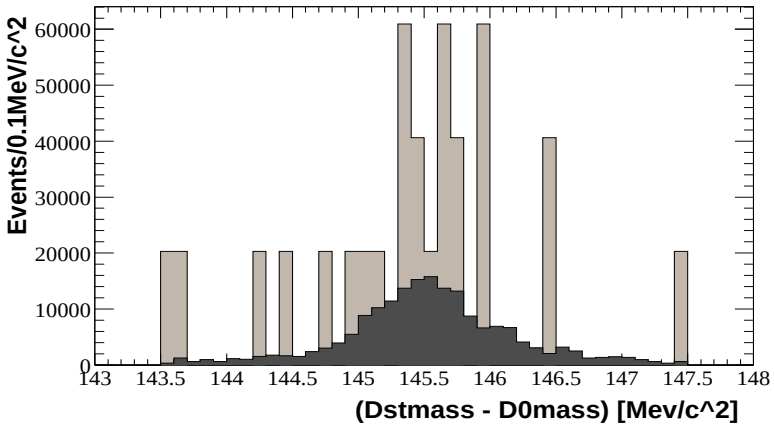

Figure 1: D^* - D^0 mass difference. The dark grey area represents the correctly reconstructed $B_d^0 \rightarrow D^{*-}\pi^+$ signal events and the light grey area represents the $b\overline{b}$ background that pass all optimised selection criteria with the exception of the (D^* - D^0) mass difference cut, which has not yet been applied.

Figure 1 shows the scaled[9] correctly reconstructed $B_d^0 \rightarrow D^{*-}\pi^+$ signal and $b\overline{b}$ background data samples that passed all optimised selection cuts with the exception of the 143.75 MeV/c^2 < (D^* - D^0) < 147.25 MeV/c^2 mass difference cut, which has not yet been applied. The distribution of both the remaining signal and the $b\overline{b}$ data samples are peaked suggesting that much of

[9]Both the signal and $b\overline{b}$ background data samples have been scaled to the expected annual yield.

the $b\overline{b}$ data sample that passes the optimised selection criteria contains true D^* candidates.

3.3.2 The B_d^0 z–vertex Selection Cut

Demanding the reconstructed B_d^0 particle to be detached from the primary vertex proves to be an effective cut in the rejection of combinatorial background. This criterion corresponds to the displaced secondary vertex trait typical of a B–decay owing to the relatively long lifetime of the B–meson.

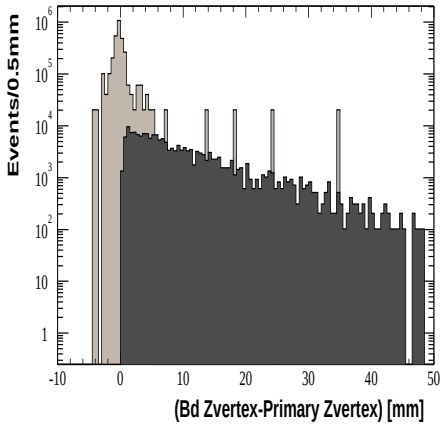

Figure 2: B_d^0 z–vertex position - primary z–vertex position. The dark grey area represents the correctly reconstructed $B_d^0 \rightarrow D^{*-}\pi^+$ signal events and the light grey area represents the $b\overline{b}$ background that pass all optimised selection criteria with the exception of the B_d^0 z–vertex position - 1^0 z–vertex position selection cut, which has not yet been applied.

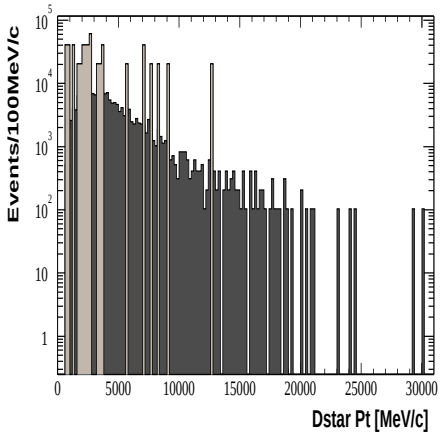

Figure 3: D^* transverse momentum distribution. The dark grey area represents the correctly reconstructed $B_d^0 \rightarrow D^{*-}\pi^+$ signal events and the light grey area represents the $b\overline{b}$ background that pass all optimised selection criteria with the exception of the D^* transverse momentum selection cut, which has not yet been applied.

Figure 2 illustrates the scaled correctly reconstructed $B_d^0 \rightarrow D^{*-}\pi^+$ signal and $b\overline{b}$ background data samples that pass all optimised selection cuts with the exception of the 1 mm $< B_d^0$ z–vertex position - 1^0 z–vertex position $<$ 50 mm selection cut, which has not yet been applied. It is evident that much of the remaining $b\overline{b}$ background is from the primary vertex. This cut eliminates a significant amount of this contribution. The $b\overline{b}$ background B_d^0 z–vertex position - 1^0 z–vertex position distribution has a long tail, which can be attributed to true B–mesons in the data sample.

3.3.3 D^* Transverse Momentum Selection Cut

The D^* transverse momentum selection cut proved to be an effective means in the rejection of the $b\overline{b}$ background with little cost to the signal level. The cut in isolation was shown to reduce the background by 44.5% with a 4% loss in signal.

Figure 3 demonstrates the scaled correctly reconstructed $B_d^0 \rightarrow D^{*-}\pi^+$ signal and $b\overline{b}$ background data samples that pass all optimised selection cuts with the exception of the D^* Pt > 1400 MeV/c selection cut, which has not yet been applied.

4 Reconstruction Results

All numbers quoted on subsequent figures refer to candidates not events. There was a Monte Carlo signal sample of 49.5k events generated. An event refers to one simulated proton–proton collision at the LHC that contains at least one $B_d^0 \rightarrow D^{*-}\pi^+$ decay. Candidates refer to the number of B_d^0 particles that were reconstructed by the analysis over the full signal sample of 49.5k events. In a few cases more than one B_d^0 candidate has been reconstructed per event. This has been attributed to double counting in the signal sample due to ghost tracks. The number of candidates and events with a reconstructed signal decay found by this analysis is summarised at the end of section 4.2.

4.1 The D^0 and D^* Reconstruction

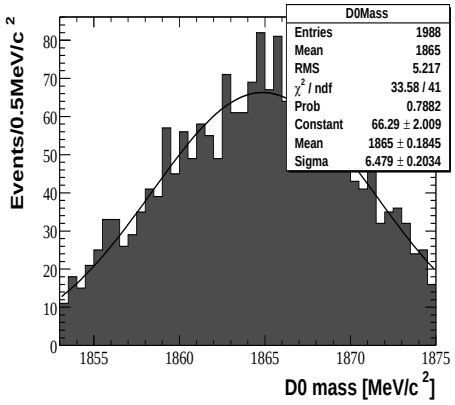

Figure 4: A D^0 mass resolution of 6.5±0.2 MeV/c^2 is achieved with this analysis.

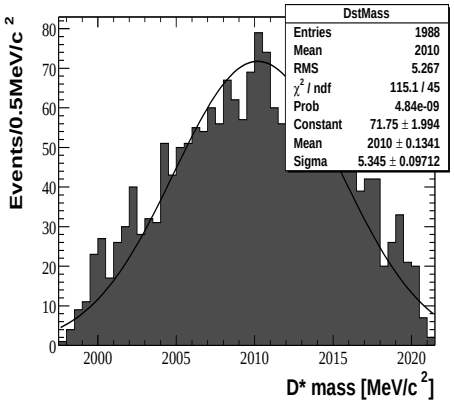

Figure 5: A D^* mass resolution of 5.4±0.1 MeV/c^2 is achieved with this analysis.

4.1.1 Slow Pion Track Studies

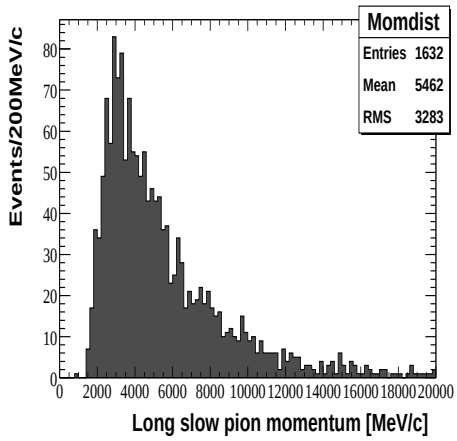

Figure 6: Momentum distribution for correctly reconstructed slow pions with long tracks.

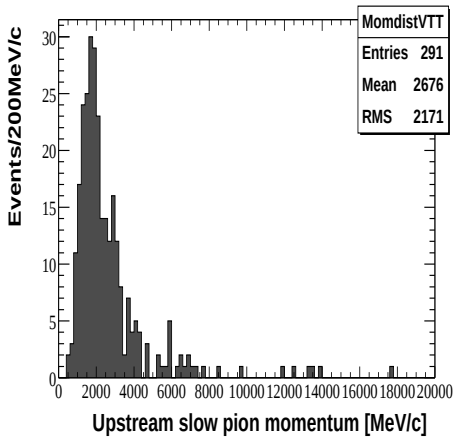

Figure 7: Momentum distribution for correctly reconstructed slow pions with upstream tracks.

Figures 6 and 7 illustrate the momentum distribution of the reconstructed slow pions according to track type. It is evident that the upstream track slow pions, figure 7, generally have a lower momentum than the long track slow pions. The typical value of momentum for a long slow pion is $\sim$5 GeV/c whereas the upstream slow pions have a lower typical momentum value of $\sim$2 GeV/c.

Including the upstream track category for slow pions has increased the yield of the reconstructed B_d^0 candidates by $\sim$15%. Only the slow pions are allowed to be reconstructed as an upstream track. Typically the other particles of the decay $B_d^0 \to D^{*-}\pi^+$ will not have a momentum comparable with the slow pion and therefore the long track definition is sufficient for all other particles in the reconstruction. Within the statistical sample investigated, the inclusion of upstream tracks for the slow pions did not cause the B/S level to rise.

The momentum and angular resolutions of the slow pions for each track category has been investigated. Figures 8 and 9 show that the momentum resolution for a upstream slow pion is approximately a factor of ten worse than the momentum resolution of a long slow pion. This is due to the smaller B–field integral of the upstream slow pion in comparison to that of the long slow pion.

The polar angular resolution of the slow pions, illustrated in figures 10 and 11, worsens from (0.52 ± 0.01)mrad to (0.91 ± 0.07)mrad when the pion

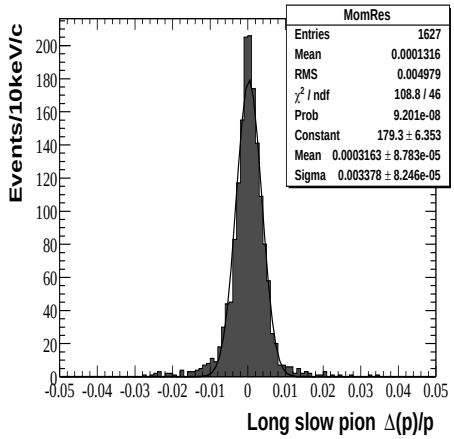

Figure 8: $\Delta p/p$ for all reconstructed slow pions with long tracks.

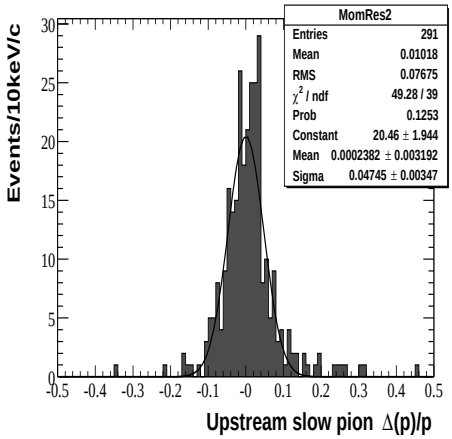

Figure 9: $\Delta p/p$ for all reconstructed slow pions with upstream tracks.

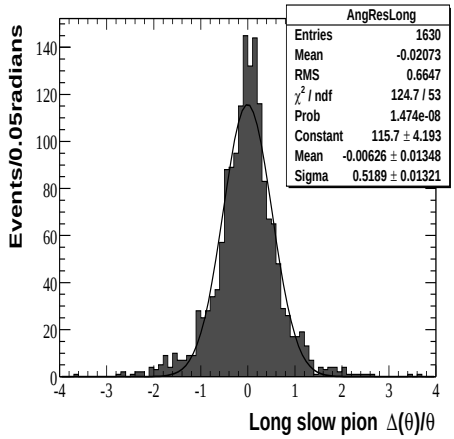

Figure 10: $\Delta\theta/\theta$ for all reconstructed slow pions with long tracks.

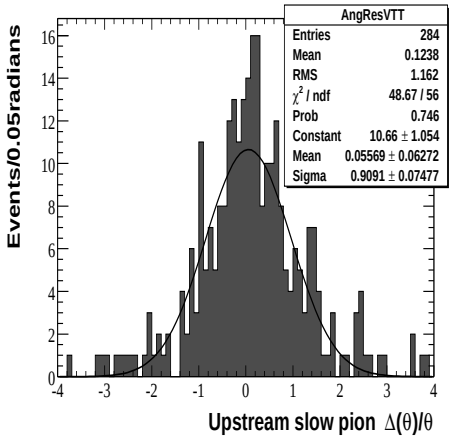

Figure 11: $\Delta\theta/\theta$ for all reconstructed slow pions with upstream tracks.

is upstream rather than long. This small degradation in angular resolution is expected as it is determined by the hits in the VELO that are close to the interaction point.

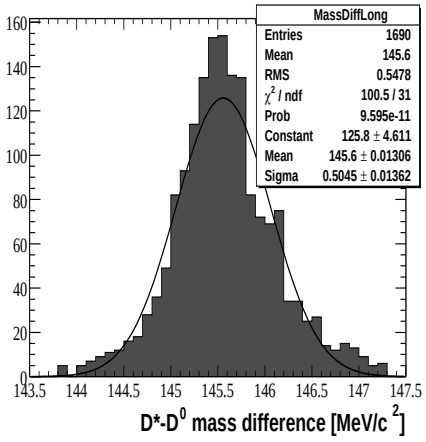

Figure 12: D^*-D^0 mass difference for all reconstructed long slow pion momenta.

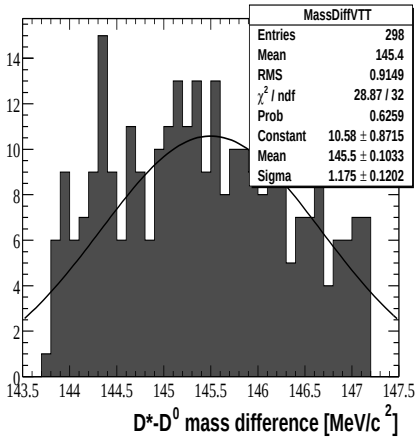

Figure 13: D^*-D^0 mass difference for all reconstructed upstream slow pion momenta.

The mass difference between the D^* and the D^0 candidates provides a powerful cut for the rejection of the combinatorial $b\overline{b}$ background. Figures 12 and 13 demonstrate the D^*-D^0 mass difference resolution for the two slow pion track categories; long and upstream. The Gaussian character of the long track mass difference is evident however due to the limited number of statistics in the upstream slow pion track category, the Gaussian spread in figure 13 is not obvious. The factor ten increase in slow pion momentum resolution is not reflected in the D^*-D^0 mass difference resolution. This worsens only by approximately a factor 2 from (0.50 ± 0.01) MeV/c^2 for long tracks to (1.2 ± 0.1) MeV/c^2 for upstream tracks owing to the relatively small increase in polar angle resolution.

4.2 The B_d^0 Reconstruction

The B_d mass resolution achieved with this analysis is 15.3 ± 0.3 MeV/c^2 as shown in figure 14. Figure 15 demonstrates the effect of the Level–0 (L0) and Level–1 (L1) trigger decisions on the signal level.

From the full signal sample of 49.5k events, 1926 signal events were reconstructed in the tight mass window. 1890 of these selected events have been identified via the Monte Carlo truth as correctly reconstructed exclusive $B_d^0 \to D^{*-}\pi^+$ decays. This gives a Monte Carlo association efficiency on

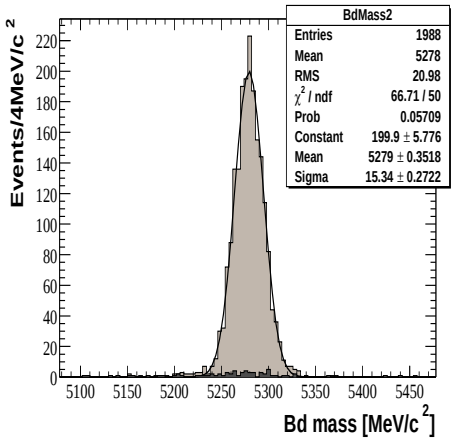

Figure 14: Distribution of the reconstructed mass of B_d candidates selected from signal events with a resolution of 15.3 ± 0.3 MeV/c^2. The light grey area represents the correctly reconstructed B_d candidates and the dark grey represents the B_d candidates incorrectly reconstructed by the algorithms.

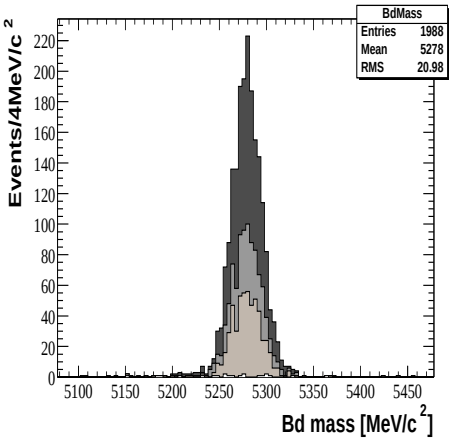

Figure 15: Distribution of the reconstructed mass of B_d candidates selected from signal events with the trigger decisions illustrated. The dark grey area represents all the reconstructed B_d candidates, middle grey represents the B_d candidates that pass the L0 trigger decision, light grey represents the B_d candidates that pass the L1 trigger decision and the white area represents those B_d candidates that pass the L0 and L1 triggers and are incorrectly reconstructed.

selected signal events of 98.1%[10]. The effect of the L0 and L1 trigger decisions on the signal level has also been analysed and is summarised in table 1.

4.3 Inclusive $b\overline{b}$ Analysis

Figure 16 shows that 24 background events[11] are selected in the loose mass window from the $b\overline{b}$ sample. 11 of these 24 events have been identified as

[10] 1968 signal events were selected in the loose mass window. 1903 of these events have been associated to Monte Carlo truth giving an association efficiency of 96.7%.

[11] *N.B* These 24 events correspond to the events from half of the $b\overline{b}$ data sample that pass all optimisation criteria. Half of the data sample was reserved in order to provide an unbiased test of the selection cuts.

	Loose Mass Window		Tight Mass Window	
	Candidates	Events	Candidates	Events
Selected	1988	1968	1942	1926
Pass L0	971	964	948	943
Pass L1	545	541	531	528
Pass L0, pass L1, false	21	21	15	15

Table 1: Summary of the number of candidates and events selected from signal events and the effect of the L0 and L1 trigger decisions on the signal level.

correctly reconstructed $B_d^0 \to D^{*-}\pi^+$ decays leaving 13 background events. The character of these 24 events have been analysed and are summarised below:

- Eleven events are correctly reconstructed $B_d^0 \to D^{*-}\pi^+$ decays.
- Five events are incomplete reconstructions such as $B_d^0 \to (D^{*-} \to (D^0 \to K^+\pi^-)\ \pi^-)\ (\rho^+ \to \pi^+\pi^0)$ where the reconstructed fast pion is from the ρ decay. This type of decay will always have a reconstructed mass below the B_d^0 mass but is selected due to the loose B_d^0 mass window. These events should not be defined as background.
- Two events have a true D^{*+} but a fake or unrelated fast pion. One event is in fact a signal event that is wrongly reconstructed and also should not be counted as background.
- Two events have a true D^0, a fake or unrelated slow pion and a true fast pion for example $B^- \to (D^{*0} \to (D^0 \to \text{K-}\pi^+)\ \gamma)\ \pi^-$ where the γ is missed and replaced by an unrelated slow pion.
- One event has a true D^0 but is otherwise a combinatorial error.
- Three selected background events are completely combinatoric.

To estimate the background in the tight mass window it can thus be assumed that there are 7 events in the loose mass window with a flat distribution across the loose mass window.

Figure 17 and table 2 summarises the effect of the L0 and L1 triggers on the 24 events selected from the combinatorial $b\overline{b}$ data sample.

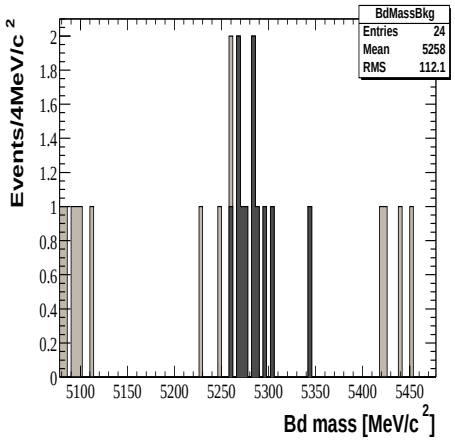

Figure 16: Distribution of the reconstructed mass of the B_d candidates selected from the $b\overline{b}$ sample. The light grey area represents the background B_d candidates and the dark grey area represents the correctly reconstructed B_d candidates from the $b\overline{b}$ data sample.

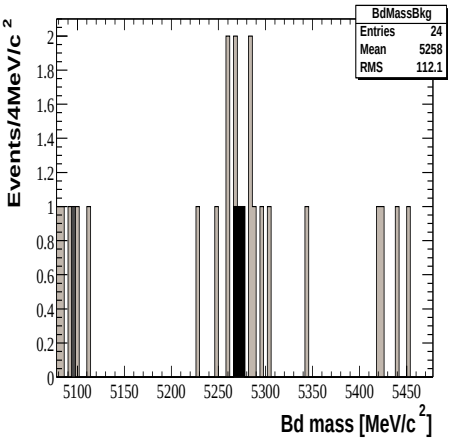

Figure 17: Distribution of the reconstructed mass of the B_d candidates selected from the $b\overline{b}$ sample with the trigger decisions illustrated. The light grey area represents all the reconstructed B_d candidates, dark grey represents the B_d candidates that pass the L0 and L1 trigger decisions and the black area represents those B_d candidates that pass the L0 and L1 triggers and are correctly reconstructed.

4.4 Minimum Bias Background Analysis

The complete minimum bias background sample of approximately 3x10^7 events was analysed using the optimised selection cuts and the loose B_d^0 mass window cut. No events were selected from this data sample.

4.5 Reconstruction Efficiency

To calculate the efficiency of the offline selection algorithms, it was necessary to access the Monte Carlo truth information of the complete signal data sample and the $B_d^0 \rightarrow D^{*-}\pi^+$ decays reconstructed by the selection algorithms. This was required in order to determine the maximum number of events that would have been reconstructed, if the selection algorithms were 100% efficient and to associate the reconstructed $B_d^0 \rightarrow D^{*-}\pi^+$ signal decays to the Monte Carlo truth. This information is summarised in table 3.

	Loose Mass Window		Tight Mass Window	
	Candidates	Events	Candidates	Events
Selected	24	24	13	13
Pass L0	9	9	5	5
Pass L1	4	4	3	3
Pass L0, pass L1, false	1	1	0	0

Table 2: Summary of the number of candidates and events selected and the effect of the L0 and L1 trigger decisions on the level of selected inclusive $b\overline{b}$ events.

#analysed	#rec'able	#rec'ted	#rec'able & #rec'ted
49.5k	13082	10396	10163

Table 3: Summary of the Monte Carlo reconstruction results of the signal $B_d^0 \to D^{*-}\pi^+$ Monte Carlo data sample.

Rec'able represents the number of events with a true Monte Carlo signal decay that is reconstructible[12], rec'ted is the number of events with a true Monte Carlo signal decay that is reconstructed[13] and rec'able & rec'ted defines the number of events that have a true Monte Carlo signal decay that are both reconstructible and reconstructed.

4.6 Computation of Annual Signal Yield

The number of $B_d^0 \to D^{*-}\pi^+$ signal decays, N_{prod}, produced in 4π in one year at LHCb assuming a visible branching fraction of 0.71×10^{-4} [14] is determined

[12]A Monte Carlo particle is reconstructible if it is associated to a protoparticle. Protoparticles are the end product of the reconstruction process. They have links to charge, kinetic and PID hypothesis information.

[13]A Monte Carlo particle is reconstructed if it fulfils the requirements of a track category; long, upstream or downstream.

[14]The visible branching fraction is calculated from the product of the individual branching fractions of the exclusive decay:

$$BR_{total} = BR(B_d^0 \to D^{*-}\pi^+) \times BR(D^{*-} \to \overline{D^0}\pi^-) \times BR(\overline{D^0} \to K^+\pi^-) \quad (1)$$

$$\Rightarrow BR_{total} = (2.76 \pm 0.21) \times 10^{-3} \times (67.7 \pm 0.5) \times 10^{-2} \times (3.80 \pm 0.09) \times 10^{-2} \quad (2)$$

$$BR_{total} = (0.71 \pm 0.04) \times 10^{-4} \quad (3)$$

by the following equation:

$$N_{prod} = pp \times pp \rightarrow bb \times bb \rightarrow b \times b \rightarrow B_d^0 \times BR \tag{4}$$

where pp is the integrated luminosity, $pp \rightarrow bb$ is the inclusive $b\overline{b}$ production cross section, $bb \rightarrow b$ is the number of b–quarks in $b\overline{b}$ events and $b \rightarrow B_d^0$ is the production fraction of B_d mesons from a b–quark.

pp	$pp \rightarrow bb$	$bb \rightarrow b$	$b \rightarrow B_d^0$	N_{prod}
$2 \times 10^{12} mb^{-1}$	$0.5mb$	2	0.391 ± 0.013	$(56 \pm 5) \times 10^6$

Table 4: Summary of factors determining the annual signal yield of $B_d^0 \rightarrow D^{*-}\pi^+$ in 4π at LHCb.

The total signal efficiency is calculated from the fraction of events that contain a signal B–decay, which are triggered, reconstructed and selected with the offline cuts. It is determined from the product of various factors:

$$\varepsilon_{tot} = \varepsilon_{det} \times \varepsilon_{rec/det} \times \varepsilon_{sel/rec} \times \varepsilon_{trg/sel} \tag{5}$$

where ε_{det} is the detector efficiency taking into account of the geometrical acceptance in 4π and all material effects of the detector, $\varepsilon_{rec/det}$ is the reconstruction efficiency of detected events, which includes the track finding efficiency, $\varepsilon_{sel/rec}$ represents the efficiency of the offline selection cuts of the reconstructed events and $\varepsilon_{trg/sel}$ is the combined L0+L1 efficiency of offline–selected events.

ε_{det}	$\varepsilon_{rec/det}$	$\varepsilon_{sel/rec}$	$\varepsilon_{trg/sel}$	ε_{tot}
9.38 ± 0.09	77.7 ± 0.4	18.5 ± 0.4	27.4 ± 1.0	0.370 ± 0.016

Table 5: Summary of the detector, reconstruction and trigger percentage fractions determining the signal efficiency for the $B_d^0 \rightarrow D^{*-}\pi^+$ decay mode.

The expected untriggered annual signal yield of the exclusive $B_d^0 \rightarrow D^{*-}\pi^+$ decay mode can be computed using:

$$N_{sel} = \varepsilon_{sel} \times N_{prod} \tag{6}$$

where N_{prod} is the number of signal decays produced in 4π in one year and ε_{sel} is the offline efficiency that takes into account of the detector acceptance, reconstruction and selection efficiencies,

$$\varepsilon_{sel} = \frac{N_{reco}}{N_{sim}} \times \varepsilon_b \tag{7}$$

$$\Rightarrow \varepsilon_{sel} = \frac{1926}{49500} \times (0.3471 \pm 0.0003) = (0.0135 \pm 0.0003) \quad (8)$$

where ε_b is the efficiency of the generator level cuts, 0.3471 ± 0.0003 in 400mrad, N_{reco} is the number of $B_d^0 \to D^{*-}\pi^+$ decays reconstructed by the selection algorithms in the tight mass window and N_{sim} is the number of Monte Carlo signal events on tape.

$$\Rightarrow N_{sel} = (0.0135 \pm 0.0003) \times (56 \pm 5) \times 10^6 = (750 \pm 17)k \text{ events} \quad (9)$$

N_{sel} can be used to determine the expected annual untagged and triggered signal yield, N_{phys}, at LHCb:

$$N_{phys} = N_{sel} \times \varepsilon_{trg/sel} \quad (10)$$

$$N_{phys} = (750 \pm 17) \times 10^3 \times (0.274 \pm 0.01) = (206 \pm 9)k \text{ events} \quad (11)$$

where N_{sel} is the untriggered annual signal yield, which is the product of N_{prod} and ε_{sel} and $\varepsilon_{trg/sel}$ is the L0 and L1 trigger efficiency of offline selected events:

$$\varepsilon_{trg/sel} = \varepsilon_{L0/sel} \times \varepsilon_{L1/sel} \quad (12)$$

$$\Rightarrow \varepsilon_{trg/sel} = (49.0 \pm 1.1)\% \times (56.0 \pm 1.6)\% = (27.4 \pm 1.0)\% \quad (13)$$

N_{prod}	ε_{sel}	N_{sel}	$\varepsilon_{trg/sel}$	N_{phys}
$(56 \pm 5)M$	$(1.35 \pm 0.03)\%$	$(750 \pm 17)k$	$(27.4 \pm 1.0)\%$	$(206 \pm 9)k$

Table 6: Summary of factors determining the annual untagged signal yield of $B_d^0 \to D^{*-}\pi^+$ decays.

4.7 Computation of the Background–to–Signal Ratio

The number of inclusive $b\overline{b}$ pairs, N'_{prod}, produced in 4π in one year at LHCb is determined by the following equation:

$$N'_{prod} = pp \times pp \to bb \quad (14)$$

$$N'_{prod} = 2 \times 10^{12} mb \times 0.5 mb^{-1} = 10^{12} \ b\overline{b} \text{ pairs} \quad (15)$$

where pp is the integrated luminosity and $pp \to bb$ represents the inclusive $b\overline{b}$ production cross section given in table 4

A Monte Carlo data sample of $\sim 10^7$ inclusive $b\overline{b}$ pairs was generated, which corresponds to $\sim$4 minutes of data taking at LHCb. Half of this

sample was used in the optimisation of selection cuts process and half of the data sample was reserved for unbiased testing of the cuts. After application of the optimised selection criteria on half of the inclusive $b\overline{b}$ data sample, 7 background events were selected as explained in section 4.3. The scaling factor to determine the number of expected annual selected background event is:

$$\frac{0.4321 \times 10^{12}}{5315600 \times 4} \approx 20300 \tag{16}$$

The factor four in the denominator takes into account of the loose–tight mass window ratio and the factor 0.4321 in the numerator is the efficiency of the generator level cuts, $\varepsilon_{bb} = 0.4321 \pm 0.0004$. The B/S ratio for the $B_d^0 \rightarrow D^{*-}\pi^+$ decay channel before tagging and triggering calculated at a 90% upper confidence limit based on Poisson statistics is therefore:

$$\frac{11.77 \times 20300}{750000} \approx 0.3 \;\; 90\% \; C.L \tag{17}$$

5 Future Developments

Since the decay mode $\overline{D^0} \rightarrow K^+\pi^-$ has a branching fraction of only $(3.80 \pm 0.09)\%$ [8], it is planned to include more decay modes of the D^0 to the exclusive analysis in order to improve the statistics and therefore the potential for this channel.

In parallel to the work with the exclusive $B_d^0 \rightarrow D^{*-}\pi^+$ decay mode, an inclusive reconstruction method has been developed where all the decays of the $\overline{D^0}$ are reconstructed, provided the decay involves at least two charged particles. This analysis method does not explicitly reconstruct the D^{*-} and uses only the fast pion from the B_d^0 decay and the slow pion from the D^{*-} decay to determine the B_d^0 4–momentum and decay time [9]. A preliminary study has indicated that the annual $B_d^0 \rightarrow D^{*-}\pi^+$ yield at LHCb can be increased by a factor 4 by the additional use of the inclusive selection.

6 Conclusions and Summary

The reconstruction of the exclusive $B_d^0 \rightarrow D^{*-}\pi^+$ decay using the LHCb software framework, DaVinci, has shown that an annual untagged and triggered signal yield of (206 ± 9) k events and a combinatorial $b\overline{b}$ background–to–signal ratio of less than 0.3 before trigger can be expected[15]. The inclusion of the

[15]The background–to–signal ratio was calculated using both the normalised signal $B_d^0 \rightarrow D^{*-}\pi^+$ and the $b\overline{b}$ background reconstruction results.

upstream tracks for the slow pion has increased the expected signal yield by approximately 15%. The forecast annual yield of $B_d^0 \to D^{*-}\pi^+$ events is expected to increase with the addition of other D^0 decay modes.

References

[1] LHCb Technical Proposal: *CERN–LHCC–98–004* 20^{th} *February 1998*

[2] 'Evaluation of the LHCb RICH Detectors and a Measurement of the CKM Angle γ': *Jonas Rademacker, CERN–Thesis–2001–017, Chapter 1*

[3] 'Asymmetry between Inclusive Charmed and Anticharmed Modes in B^0–$\overline{B^0}$ Decays as a Measurement of CP Violation': *I. Dunietz and R.G. Sachs, Phys. Rev. D37, 3186 (1988)*

[4] 'Sensitivity with $B_s^0 \to h^+h^-$ Decays at LHCb': *G. Balbi et al, CERN–LHCb–2003–124*

[5] http://lhcb-comp.web.cern.ch/lhcb-comp/bookkeeping/: *LHCb Bookkeeping Webpage*

[6] LHCb Reoptimized Detector Design and Performance: *CERN–LHCC–2003–030* 9^{th} *September 2003*

[7] http://lhcb-comp.web.cern.ch/lhcb-comp/Reconstruction/default.htm: *LHCb Brunel–The LHCb Reconstruction Program Webpage*

[8] 'Review of Particle Physics' Phys. Rev. D 66, 010001 (2002) *K. Hagiwara et al*

[9] 'Evaluation of the LHCb RICH Detectors and a Measurement of the CKM Angle γ': *Jonas Rademacker, CERN–Thesis–2001–017, Chapter 3*